



International Journal of Heavy Vehicle Systems

ISSN online: 1741-5152 - ISSN print: 1744-232X

<https://www.inderscience.com/ijhvs>

Stress analysis of an air tube bracket on a heavy-duty commercial vehicle's chassis

Paşa Yayla, Burak Ateş, Ozan Berke Yabar

DOI: [10.1504/IJHVS.2023.10057365](https://doi.org/10.1504/IJHVS.2023.10057365)

Article History:

Received:	11 July 2021
Accepted:	16 December 2021
Published online:	06 July 2023

Stress analysis of an air tube bracket on a heavy-duty commercial vehicle's chassis

Paşa Yayla*

Mechanical Engineering Department,
Marmara University,
34840 Istanbul, Turkey
Email: pasa.yayla@marmara.edu.tr
*Corresponding author

Burak Ateş

Calculation and Simulation Department,
Mercedes-Benz Türk A.Ş.,
34522 Istanbul, Turkey
Email: burak.ates@daimlertruck.com

Ozan Berke Yabar

Mechanical Engineering Department,
Marmara University,
34840 Istanbul, Turkey
Email: ozanberkeyabar@gmail.com

Abstract: This study is performed on the air tube bracket system of a heavy-duty commercial truck oscillating at its natural frequency under dynamic load exposed from all along its route. The dynamic analysis of the bracket with the entire commercial vehicle is made based on the data from rough road conditions. In all studies, the finite element models are created with the Medina software, and the solving process is performed with the Permas software. The results of the current work provided not only the optimum geometry of the air tube bracket system of a heavy-duty truck but also its ideal dimensions. The analysis also revealed that in addition to the geometry the straps' width and their locations are of paramount importance in their overall performance.

Keywords: finite element analysis; air tube bracket; heavy-duty commercial vehicle; stress analysis; simulation.

Reference to this paper should be made as follows: Yayla, P., Ateş, B. and Yabar, O.B. (2023) 'Stress analysis of an air tube bracket on a heavy-duty commercial vehicle's chassis', *Int. J. Heavy Vehicle Systems*, Vol. 30, No. 1, pp.17–35.

Biographical notes: Paşa Yayla received his BSc and MSc degrees in Mechanical Engineering from Istanbul Technical University, and a PhD degree in Mechanical Engineering from Imperial College of Science, Technology,

and Medicine, London, UK. He has been working as a Professor in Mechanical Engineering Department at Marmara University. His research interest focuses on fracture mechanics of polymers and polymer composites and failure analysis of engineering materials.

Burak Ateş received his BSc degree in Mechanical Engineering Department from Marmara University, Istanbul Turkey, and his MSc in Mechanical Engineering Department at the Technical University of Braunschweig – Germany. He is currently working as a Senior CAE Engineer at Calculation and Simulation Department, Mercedes-Benz Türk A.Ş., Istanbul, Turkey.

Ozan Berke Yabar received his BSc degree in Mechanical Engineering from Marmara University and MEng degree in Automotive Engineering from Esslingen University. Previously, he worked at Daimler Truck and Volvo Group. Now, he is working as an NVH Engineer at EDAG Engineering Scandinavia AB, Sweden. His research interest focuses on structural dynamics, mechanical vibrations, and NVH applications in automotive systems.

1 Introduction

Trucks are heavy-duty vehicles intended to carry freight. Depending on the working purposes, logistics companies may request different levels of compressed air or high fuel tank capacity. Air tubes and fuel tanks are mounted on the chassis with brackets. As the volume of these tubes is increased, the amount of stress on the brackets increases. In such operations, failure of the bracket that holds the air tube is a common problem in vehicle development. There are a number of studies on the design and optimisation of these kinds of brackets.

Depending on the design requirements, different design strategies, i.e., shape, size, and topology optimisation, are extensively employed. Walunje and Kurkute (2013) studied the use of lightweight material for a bracket to reduce weight. Ghorpade et al. (2012) have designed the engine mounting bracket of a car and focused on determining the natural frequencies. Naghate and Patil (2012) developed an engine mounting bracket aiming to reduce noise and vibrations. It was pointed out that the bracket should be designed to keep the resonance frequency (or frequencies) out of the operating range. In his work on designing large commercial vehicles, Chang (2006) has studied various optimisation methods to attempt for optimal design considering sound durability, safety, noise, vibration, and harshness (NVH) characteristics, especially in the design of suspension control arm and mount bracket.

It is highly important that these brackets have to provide proper stiffness, eigenfrequency, strength, and cost to comply with the durability and NVH requirements. An air tube bracket is a rather small component compared to the entire chassis. However, any failure or lack of a proper design in this part may have detrimental consequences on the entire safety of the vehicle.

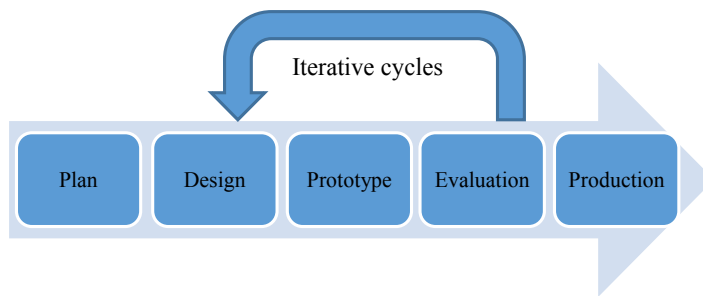
In the present work, an air tube bracket on a chassis that oscillates at its natural frequency under dynamic loads is examined. Because of this oscillation, the maximum stress on the bracket is reduced with the newly designed and optimised tube bracket system.

2 Computer-aided engineering

In vehicle development, physical tests are mandatory for verification of the final product design. Today's biggest challenge for automotive manufacturers is how to reduce product development time and testing costs. In the automotive industry, to reduce these tests, development costs, and time, Computer-Aided Engineering (CEA) techniques are often used (Chang et al., 2009; Bakır et al., 2018).

There is a general conventional development procedure for mechanical products shown in Figure 1 (Kojima, 2000). From a plan to production, all mechanical products follow these steps. During the experimental evaluation step, the product can go back to the design steps according to the test results.

Figure 1 Conventional development procedure (see online version for colours)



Source: Kojima (2000)

It is quite common in engineering practice that the competitive product appears after repeated failures in experiments. The CAE could be accepted as numerical experiments in design steps. In automotive engineering, engineers employ CAE in order to simulate crashworthiness, drivability, durability, strength and NVH (Kojima, 2000; Cho et al., 2007; Raffaldini, 2012).

3 Finite element analysis

Many of the physical phenomena in engineering can be defined with differential equations. When these equations cannot be solved analytically, the finite element method (FEM) is utilised to solve them. The FEM is a numerical approach to solving these differential equations. For a given load, engineering stress, strain, and other related parameters of structures can be calculated.

In static analysis, it is assumed that the loads applied to the object are fixed or the applied load is acting slowly and remains constant at a certain point. Because of this assumption, the acceleration of each region in the model is considered to be zero. As a result, the static analysis ignores the inertial and damping forces. Dynamic analyses are more reliable for validation studies because situations like static analysis are not often encountered in real life. If the frequency of the applied load is greater than 30% of the lowest frequency, dynamic analysis is recommended.

In dynamic analysis, the loads are divided into two main categories: deterministic and non-deterministic ones. Deterministic loads are functions of time and can therefore be estimated. These can be classified as harmonic, periodic, or non-periodic. The type of results also determines the type of loads (Polat, 2019). If deterministic loads are used, the results will also be deterministic. Non-deterministic loads are found by statistical methods since they are not a function of time. Typical dynamic loads encountered in engineering are harmonic, periodic, shock, and general loadings (Yay and Ereke, 2003; Lonny et al., 2007).

3.1 Frequency analysis

Each structure has specific natural frequencies. Sometimes this natural frequency is also called the resonance frequency. Structures stimulated at their natural frequency start to vibrate at this frequency continuously. This vibration continues even after the excitement process is over. There is one specific mode shape for each natural frequency. These mode shapes show how the structure vibrates at this frequency. By looking at the mode shapes, it can be analysed in which parts of the structure improvements can be made. In a structure that vibrates at its natural frequency, huge stresses and displacements are observed. In such cases, dynamic analysis methods should be used to analyse the structure.

Studies can be conducted to prevent resonance with the dynamic analysis. The mode shapes corresponding to the natural frequencies obtained as a result of dynamic analysis depend on the material properties and the geometries of the parts.

3.2 Free vibration analysis

Natural frequencies and mode shapes of the engineering structures are obtained by free vibration analysis. The mathematical expression of undamped free vibration analysis is as follows (Yang, 1991);

$$[M]\{\ddot{x}\}+[K]\{x\}=\{0\} \quad (1)$$

In equation (1), M represents the mass matrix, K is the stiffness matrix, x is the displacement, and \ddot{x} is the acceleration. It is assumed that there is a harmonic motion to solve this equation.

$$\{x(x,y,z,t)\}=\{\Phi(x,y,z)\}\sin\omega t \quad (2)$$

Here $\{\Phi\}$ denotes eigenvector or free vibration patterns, and ω circular frequency. This solution shows that all degrees of freedom of the vibrating structure move in harmony with each other. When the equation used for the solution is placed in the original equation, the equation can be simplified as follows.

$$-\omega^2 [M]\{\Phi\}\sin\omega t+[K]\{\Phi\}\sin\omega t = 0 \quad (3)$$

$$([K] -\omega^2 [M])\{\Phi\} = 0 \quad (4)$$

There are several homogeneous mathematical operations in equations (3) and (4). With these mathematical operations, eigenvectors are obtained and these form the basis of the eigenvalue problem. As a result of these processes, the eigenvalues and eigenvectors are obtained. Thanks to these calculated parameters, the free vibration characteristics of the

parts or structures are evaluated. From the calculated natural frequency, eigenvalues are calculated by equation (5)

$$f = \frac{w}{2\pi} \quad (5)$$

The unit of the natural frequency in equation (5) is Hertz and has the natural frequency as much as the degree of freedom of the structure. The unit of the angular frequency w in equation (5) is rad/sec. The number of eigenvalues and eigenvectors is also equal to the degree of freedom of the structure.

3.3 Random vibration analysis

This type of vibration analysis is used to calculate the response of non-deterministic loads. The non-deterministic loads are used in these analyses such as loads on commercial vehicle's wheels under rough road test. In this analysis, loads are defined statistically as power spectral density functions. The units of the loads used here are obtained by dividing the frequency function's squared load by frequency.

In the software where this analysis is run, stresses and displacements are determined for a certain frequency. These values are given as root mean square. The equations of motion for a system with n degrees of freedom excited by a time-dependent load are as follows.

$$[M]\{\ddot{u}(t)\} + [B]\{\dot{u}(t)\} + [K]\{u(t)\} = \{f(t)\} \quad (6)$$

Equation sets are reduced to independent equations using coordinate transformation.

$$\ddot{x}_r(t) + 2\zeta_r w_r \dot{x}_r(t) + w_r^2 x_r(t) = m_r(t) \quad (7)$$

The node coordinates represented by x_r and u_r in equation (7) have the following relationship.

$$\{u(t)\} = [\Phi] \{x(t)\} \quad (8)$$

where $m(t)$ is the modal load vector and is calculated by the following equation.

$$\{m(t)\} = [\Phi]^T \{f(t)\} \quad (9)$$

The excitation power spectral density matrix can be shown as $[S_f(\omega)]$ and the modal force matrix is calculated as follows (Paskalov and Reese, 2003);

$$S_m(\omega) = [\Phi]^T [S_f(\omega)] [H^*(\omega)] \quad (10)$$

The matrix denoted by $[H(\omega)]$ is the modal transfer matrix and $[H^*(\omega)]$ is the conjugate matrix of this matrix in the complex plane. The power spectral density of displacement, velocity, and acceleration responses are calculated by the formulas below.

$$[S_u(\omega)] = [\Phi] [S_x(\omega)] [\Phi]^T \quad (11)$$

$$[S_{\dot{u}}(\omega)] = [\Phi] [S_{\dot{x}}(\omega)] [\Phi]^T \quad (12)$$

$$[S_{\ddot{u}}(\omega)] = [\Phi] [S_{\ddot{x}}(\omega)] [\Phi]^T \quad (13)$$

Using these equations, the mean square responses are determined from the diagonal terms of the matrices.

$$[R_u] = [\Phi] [R_x(0)] [\Phi]^T \quad (14)$$

$$[R_{\dot{u}}] = [\Phi] [R_{\dot{x}}(0)] [\Phi]^T \quad (15)$$

$$[R_{\ddot{u}}] = [\Phi] [R_{\ddot{x}}(0)] [\Phi]^T \quad (16)$$

The stresses that occur in the elements here are calculated from the displacements in the nodes.

$$\{\sigma\} = [A] \{u\} \quad (17)$$

$$\{\sigma\} = [A] [\Phi] \{x\} \quad (18)$$

The nodal displacement is denoted by $\{u\}$ and the modal displacement is denoted by $\{x\}$. $[\Phi]$ shows matrix eigenvectors and $[R_\sigma]$ shows the stress correlation matrix, which is found as follows.

$$[R_\sigma] = [W] [R_x] [W]^T \quad (19)$$

3.4 Modal time history analysis

If the loads are known to change with time and if the desired response is a function of time, a modal time history analysis should be performed. Modal analysis techniques are used to solve motion equations for multi-degree-of-freedom systems. There is a relationship between the time interval and the solution. As this interval becomes smaller, the accuracy of the solution increases.

The general motion equation of the system excited by a force based on time is as follows.

$$[M] \{\ddot{u}(t)\} + [B] \{\dot{u}(t)\} + [K] \{u(t)\} = \{f(t)\} \quad (20)$$

where $[M]$ is inertia, $[B]$ is damping, and $[K]$ is stiffness matrix and also $f(t)$ is n-dimensional force vector.

The main concern in the modal analysis is to convert the system of equations associated with using the modal matrix $[\Phi]$ as a transformation matrix into a series of independent equations (Luizelli et al., 2018);

$$[\Phi] = [\{\varphi\}_1 + \{\varphi\}_2 + \{\varphi\}_3 + \dots + \{\varphi\}_n] \quad (21)$$

$$[K] [\Phi] = [M] [\Phi] [w^2] \quad (22)$$

The expression shown as w^2 in equation (22) is the diagonal matrix of natural frequencies. This motion equation can be written as follows by associating it with the modal displacement vector $\{x\}$.

$$\{u\} = [\Phi] \{x\} \quad (23)$$

If the equation is then simplified and the displacement vector $\{u\}$ is removed from the equation and combined with the first equation of motion, equation (24) is obtained (Anselmet and Mattei, 2016):

$$[\Phi]^T [M] [\Phi] \{ \ddot{x} \} + [\Phi]^T [C] [\Phi] \{ \dot{x} \} + [\Phi]^T [K] [\Phi] \{ x \} = [\Phi]^T f(t)(t) \quad (24)$$

The modal matrix is normalised to satisfy the following three equations.

$$[\Phi]^T [M] [\Phi] = [1] \quad (25)$$

$$[\Phi]^T [C] [\Phi] = [2] [\zeta] [w] \quad (26)$$

$$[\Phi]^T [K] [\Phi] = [w^2] \quad (27)$$

Then, when equations (25)–(27) are re-arranged, and the second-order differential equation is obtained.

$$\ddot{x}_i + 2 \zeta w \dot{x}_i + w^2 x_i = \{\varphi\}_i^T \{f(t)\} \quad (28)$$

Various methods can be used to solve this equation. The most convenient one is to solve it with the step-by-step integration method. Examples are Wilson-Theta and Newmark (Zienkiewicz et al., 2013).

4 Testing

In order to make a robust and reliable design, automotive manufacturers are making a lot of tests for components separately and after all of the validated components, the vehicle is integrated and tested again entirely. In general, trucks are made for long-distance travel or construction. That is why the manufacturers are simulating the entire vehicle with the data collected from the real road conditions and the rough road testing facilities. These rough road tests, called general durability tests, help the manufacturer to see their vehicle's strengths and weaknesses.

Rough road tests are considered to meet all durability requirements for the vehicle's whole life. Depending on the vehicle and cases, rough road tests can be heavier. Rough road tests need special equipment and tracks. Because of this reason, in general, most of the manufacturers have their own rough road test facility, Figure 2.

Figure 2 Mercedes-Benz Testing and Development Center, Wörth, Germany (see online version for colours)



Source: https://www.mercedes-benz-trucks.com/de_DE/models/new-actros/reliability.html

5 Analysis of vehicle

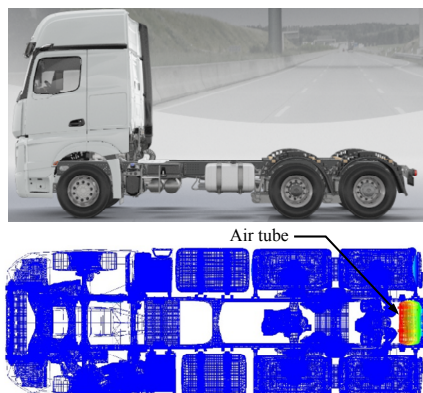
The parts analysed here are sourced from the NX library and transferred to Medina software. The finite element model analysed here is a combination of shell elements (QUAD4, TRIA3), rigid elements (RBE2, IQUAD), and mass elements (MASS6).

The connection is provided by interpolation elements used in the Permas solver program. Interpolation elements are used to build a rigid connection between nodes and elements. These elements are similar to RBE2 rigid body elements. However, RBE2 elements only enable the connection between nodes. Different from RBE2 elements, interpolation elements connect the elements to nodes rigidly. In this study, IQUAD elements are chosen among the interpolation elements.

5.1 Heavy-duty commercial vehicle

In this study, the finite element model of the heavy-duty commercial vehicle was used. In all studies, finite element models are created with the Medina software and the solution process is performed with the Permas software (INTES GmbH, 2012). The vehicle type used is the tractor, as shown in Figure 3, which also shows the location of the air tube. The total weight of these vehicles can vary from 18 to 33 tons. The wheelbase of the vehicles can vary between 3250 mm and 4000 mm.

Figure 3 Mercedes-Benz Actros 6×4 semitrailer tractor and the location of air tube (see online version for colours)



In this work, the whole commercial vehicle is simulated based on the data from rough road conditions. All analyses cover the entire vehicle, as indicated in Figure 3. The considered analysis type is transient dynamic; and since the whole vehicle is modelled, the total number of nodes is about 5 million.

5.2 Heavy-duty vehicle chassis

The chassis is a collective term for vehicles and it includes all the parts of a vehicle, except the bodywork and it includes wheels, brakes, frame, suspension systems, axles, etc. Chassis quality is an important parameter for vehicle dynamics and vehicle durability.

5.3 Chassis materials

The materials studied on the chassis in Figure 4 are mainly high-strength steel grades S500MC and S600 MC, and their properties are tabulated in Tables 1 and 2, respectively (European Committee for Standardization, 2013).

Figure 4 Mercedes-Benz Actros frame (see online version for colours)



Source: https://www.mercedes-benz-trucks.com/en_ID/models/long-distance-actros/economics-and-technics/chassis.htm

Table 1 Strength properties of S500MC steel

<i>Property</i>	<i>Value</i>
Density	7.85 t/m ³
Poisson's ratio	0.30
Tensile strength (σ_t)	820 MPa
Yield strength (σ_y)	600 MPa
Young's modulus	210 GPa

Source: European Committee for Standardization (2013)

Table 2 Strength properties of S600MC steel

<i>Property</i>	<i>Value</i>
Density	7.85 t/m ³
Poisson's ratio	0.30
Tensile strength (σ_t)	700 MPa
Yield strength (σ_y)	573 MPa
Young's modulus	210 GPa

Source: European Committee for Standardization (2013)

6 Stress analysis results

The commercial vehicle is simulated based on the data from rough road conditions. All analyses cover the entire vehicle, as indicated in Figure 3. In the first analysis, the maximum stress on the bracket was found to be 0.657 times of dynamic material limit for

the rough road conditions, Figure 5. From the eigenvalue analysis results, the critical mode shapes for the maximum stress is investigated and countermeasures are taken, Figure 6. The relative positions of the tubes, straps, and brackets are also presented in Figure 6.

Figure 5 Stress result of the original bracket (see online version for colours)

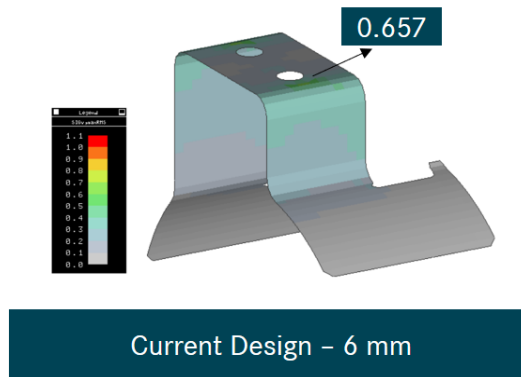
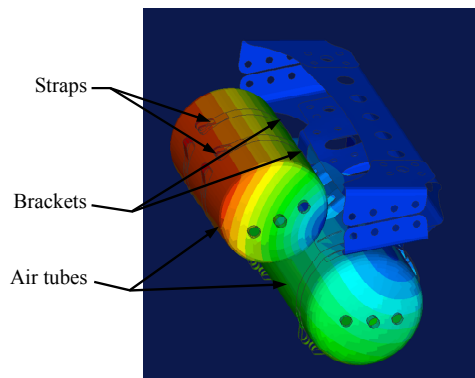


Figure 6 One of the critical mode shapes of air tube (see online version for colours)

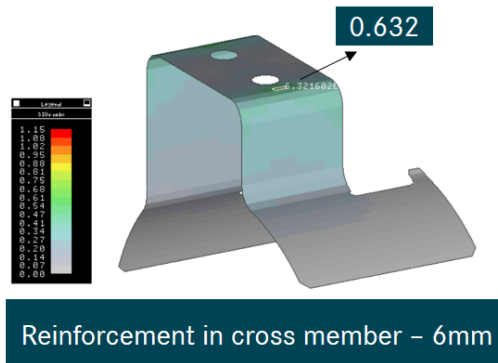


The first improvement accounts for making minor changes in the original bracket. Then in the following examples, newly designed brackets with different geometries and dimensions are proposed and simulated.

6.1 Reinforcement in cross member

In this study, an additional part was used to reduce the effect of vibration at the back of the vehicle, Figure 7. The material of the part used is the same as the part that is attached to the chassis, and its thickness is 5 mm. The part is modelled using QUAD4 elements and is integrated into the entire vehicle model in the Medina software. The part was connected to the frame with 6 M17 bolts. According to the simulation results, improvements were observed compared to the previous design.

Figure 7 Maximum stress result on the bracket with reinforcement in the cross member (see online version for colours)



In this analysis, the upper straps are placed symmetrically, and the lower straps are placed asymmetrically. The thickness of the upper band is 2.5 mm and its material is S500MC steel and the thickness of the lower band is 1.5 mm and its material is S500MC steel.

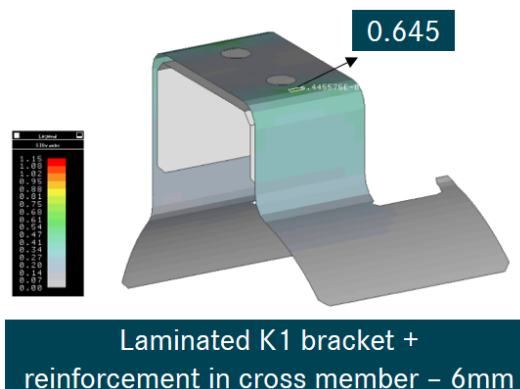
The maximum stress on the bracket dropped by about 4%. Different solutions were examined because this amount of decrease in maximum stress was below the expectations and did not comply with the requirements.

According to test results, natural frequencies have been found and 46% of the contribution on stress is from 23 Hz frequency and 19% of the contribution on stress is from 30 Hz frequency. Moreover, the production cost of the added part is to be taken into consideration.

6.2 Laminated bracket and reinforcement in cross member

In this study, an extra laminated bracket was added to reduce the stress caused by vibration at both ends of the bracket, Figure 8. Strap thicknesses were kept the same, 2.5 mm and 1.5 mm for upper and lower, respectively. Laminated reinforcement is screwed into the original bracket with M17 bolts. The stress on the bracket was higher than in the previous analysis.

Figure 8 Maximum stress result on the bracket with laminated bracket and reinforcement in the cross member (see online version for colours)

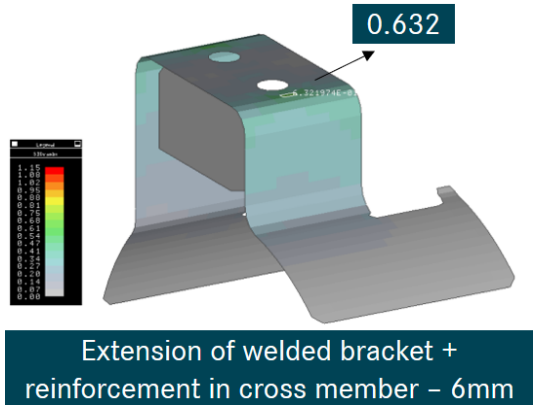


There was no major change in the natural frequency results. 23 Hz frequency 23% of contribution to stress and 30 Hz frequency 20% of contribution to stress.

6.3 Extension of welded bracket + reinforcement in cross member

In this study, the two ends of the bracket are welded with the S500MC material to reduce stress on the bracket, Figure 9. Extension of welded bracket improves durability and reduces the maximum stress on the bracket. It has increased the natural frequency, but not to the level that was targeted.

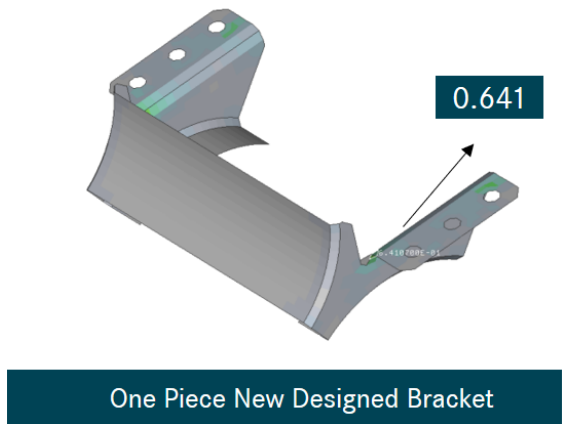
Figure 9 Maximum stress result on the bracket with the extension of welded bracket + reinforcement in the cross member (see online version for colours)



6.4 One part new designed bracket for both air tubes

The one-part bracket was designed, aiming to reduce the vibration on the chassis significantly. That newly designed bracket made from S500MC material is bolted to the frame from 4 places of 5 mm thickness, Figure 10.

Figure 10 Maximum stress result on one part new designed bracket (see online version for colours)



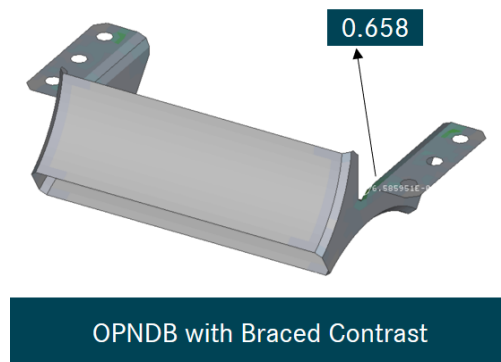
Due to the geometry of the bracket used here, all the straps are modelled with 1.5 mm thickness and QUAD4 element. According to rough road analysis results, the maximum stress on the bracket was measured as 0.641 times the dynamic material limit. Although this result is better than the original design, it still has not provided the expected performance.

The same analysis was repeated using 6 M17 bolts from 6 points instead of 4 M17 bolts, but no major changes were observed. Thus, in order to reduce the cost, a 4-bolt model was considered in the design.

6.5 One part new designed bracket for both air tubes with braced contrast

In this part of the study, the rigidity of the bracket is studied, Figure 11. The aim here is to increase the rigidity of the bracket. 1447 elements are used in this bracket modelling. In the FEM model of the bracket, standard linear shell elements TRIA3 and QUAD4 are used. The material and thickness are S500MC and 5 mm, respectively, and 4 straps of 1.5 mm thickness were used. To reduce the vibration on the frame, the lower part of the bracket is completely attached to the tubes, just like its upper part. These bonding processes were made with IQUAD elements.

Figure 11 Maximum stress result on one part new designed bracket for both air tubes with braced contrast (see online version for colours)



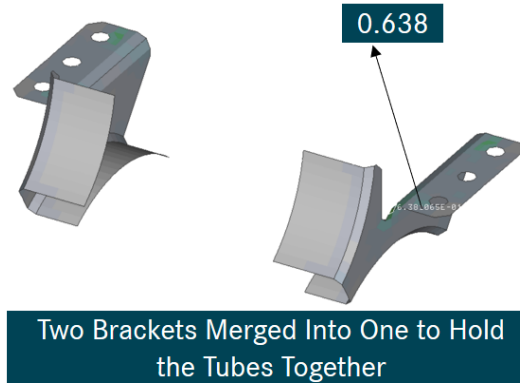
In this model, the bracket is connected to two tubes, and at the same time, the straps passing both sides of the bracket are connected to the bracket with IQUAD elements. In simulations, both 6 and 4 bolts were analysed with M17 bolts. As expected, fastening with 6 bolts did not change the maximum stress significantly.

Since the stress on the parts of the bracket connected to the tubes is approximately 10 times below the dynamic material limit and those parts are noted to be removed to reduce the weight of the part. In the next analysis, the knowledge obtained from this analysis is used.

6.6 Two brackets merged into one to hold the tubes together

In this design, the parts with low-stress values were removed from the bracket, Figure 12. This bracket is created with 768 QUAD4, 20 TRIA3 elements, and 799 nodes. The material is again S500MC and its thickness is prepared with a 5 mm shell element.

Figure 12 Maximum stress result on two brackets merged into one to hold the tubes together (see online version for colours)



The contact surface area of the bracket with the tubes decreased and the maximum stress is reduced compared to the previous design. Several further analyses were made to see how much the part thickness affects the maximum stress.

New analyses in 6, 7, and 8 mm thicknesses were made with the same bracket design, Figure 13. As a result of the dynamic analysis of the bracket, it was determined that the maximum stress decreased in proportion to the thickness of the bracket. According to the results, the 8 mm bracket is stronger, but the movement area of the bracket on the frame and the manufacturability of the bracket should also be considered.

In order to find the most optimal design for the bracket, it is necessary to look at the parts on the frame. Accordingly, the most suitable thickness is selected from both manufacturability and strength perspectives.

6.7 Effect of straps

In the original design in the series, two pairs of straps, 2.5 mm at the top and 1.5 mm at the bottom, are used, Figure 14. The thickness of the upper straps was reduced to 1.5 mm to see how much the stress on the bracket is proportional to the thickness of the strap.

According to the results of the analysis, although the 2.5 mm thickness strap is more durable, the 1.5 mm strap gave a better stress result in the rough road analysis.

With that design, the lowest maximum stress value was obtained in the welded bracket.

For this reason, the analysis continued on the welded bracket given in Figure 15. Because of their geometry, the strap thickness of the new design brackets is already 1.5 mm and they have not been analysed again.

When the analyses were repeated for the extension of the welded bracket and reinforcement in the cross member, a serious decrease in stress was observed on the bracket analysed by the same methods. Only the thickness of the strap has been reduced from 2.5 mm to 1.5 mm without changing the thickness of the part.

A 13% reduction was achieved by welding and changing the thickness of the strap without changing the thickness and material of the original bracket, Figure 16. Moreover, 7 mm thick parts with the same material and bracket are used on the frame. For this reason, the dynamic analysis of this bracket in 7 mm thickness was also performed.

Figure 13 Analysis results of 6, 7 and 8 mm brackets (see online version for colours)

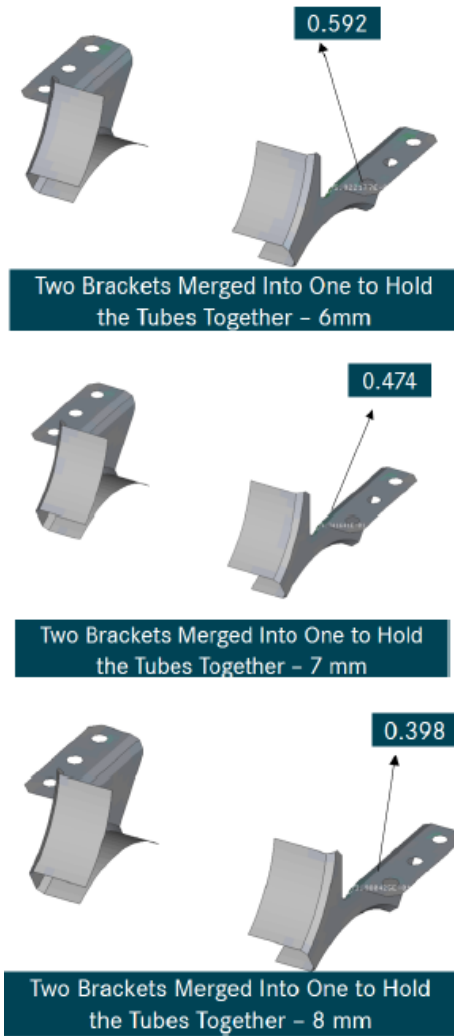


Figure 14 Original design with 1.5 mm straps (see online version for colours)

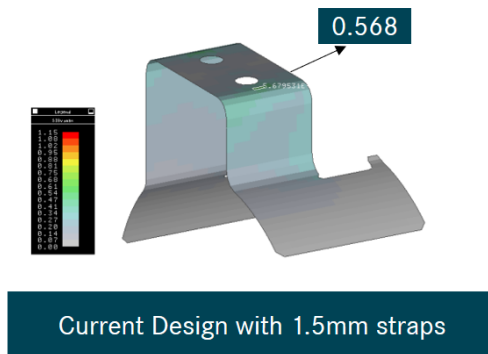


Figure 15 Maximum stress result on extension of welded bracket + reinforcement in cross member 5 mm (see online version for colours)

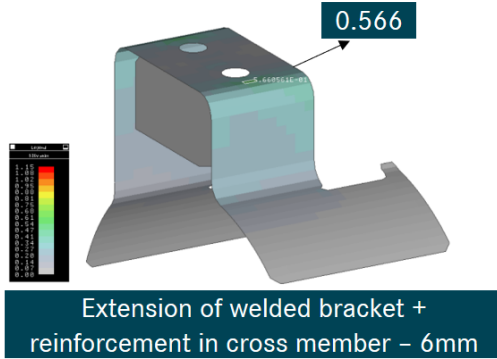
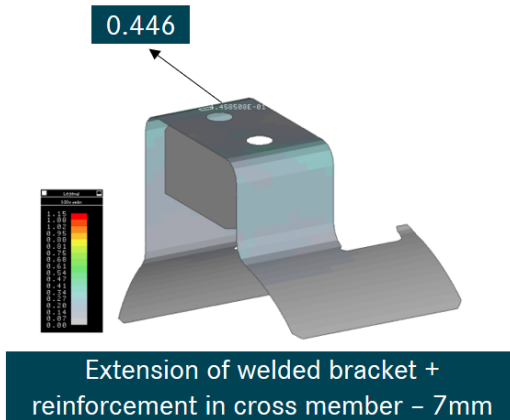


Figure 16 Maximum stress result on the extension of welded bracket and reinforcement in cross member 7 mm (see online version for colours)



7 Discussion of results

The maximum stress on the original bracket was 0.657 times higher than the dynamic material limit, as shown in Figure 5. At the beginning, this study aimed to reduce this stress level by 10%. Keeping that aim in mind, different design scenarios were considered. The main goal of these alternative designs was to reduce the maximum stress by making small changes in the original bracket. To be able to propose design adjustments, the mode shapes of the design had been examined. Additionally, precautions have been taken to adjust itself according to the movement and absorb the vibration.

Taking into consideration these design requirements, the part shown in Figure 10 was optimised. The maximum stress was reduced and distributed to other areas, with the help of the location of the maximum stress and the mode shapes that had been found after the modal analysis. On the first try, the aim was to have better contact between the bracket and the tubes. In this way, there were no considerable changes in stress, but the cost also increased. That is why it was necessary to find a better solution. The surface of the part had been expanded. Thus, the part needed to be lightened, so the areas with lower stress

have been removed. Then, the connection of the part to the chassis was examined. However, there was no connection between stress level and connection types or the number of bolts. With this part, the optimal design has been achieved, as shown in Figure 16. In the same way as the welded part, integrating the optimal width and to integrate it into the entire vehicle is left up to the vehicle manufacturer.

The optimum width is calculated as 1.5×1.5 mm. Out of this conclusion, the analyses with 2.5×1.5 mm belts are repeated, and it has been concluded with all the results that the targeted stress reduction was achieved.

Here, the lowest stress level for the 7 mm bracket was found as 0.446 and for the 6 mm bracket 0.566. The original bracket was 6 mm, so this part may be selected. However, because there are many parts on the same chassis with the same width and S500MC material, a 7 mm bracket was decided to be the most convenient thickness.

8 Conclusions

In this work, finite element stress analysis of the air tube bracket system of a heavy-duty truck is studied. The main aim is to increase the rigidity of the bracket and to reduce the maximum stress acting on it. The bracket reaches its natural frequency due to the dynamic load exposed from all along its route.

In the light of the analyses, it was clear that not only the geometry adjustments but also the width of the straps that hold the tubes and their relocations were beneficial. Furthermore, the welded design is better from a durability perspective mainly due to the fact that it not only reduces the stress level but also increases the critical mode frequency.

The lowest stress level among the alternative designs was observed on the welded bracket. The welding was successful in reducing the movement. Therefore, simulations were concentrated on the welded bracket. The necessary design adjustments were made to the original design, which was then simulated again. It is known that as a part gets wider, its stiffness level rises. However, it has to be considered that the part has contact with other parts. That is why it might not always be proper to say that wider is better.

Acknowledgement

This project would not have been possible without the support of the teams in Mercedes-Benz Türk A.Ş. The authors would like to express sincere gratitude to R&D Director Mustafa Üstertuna, manager Mehmet Bakır and his team.

This study has been funded by BAPKO of Marmara University under grant no: FEN-E-080415-0111.

References

- Anselmet, F. and Mattei, P.O. (2016) 'Wave propagation in elastic media', *Acoustics, Aeroacoustics and Vibrations*, Wiley-ISTE, pp.167–218, <https://doi.10.1002/9781119178361.ch6>

- Bakır, M., Ozmen, B. and Donertas, C. (2018) ‘Correlation of simulation, test bench and rough road testing in terms of strength and fatigue life of a leaf spring’, *Procedia Engineering*, Vol. 213, pp.303–312, <https://doi.org/10.1016/j.proeng.2018.02.031>
- Chang, H.S. (2006) *A Study on the Analysis Method for Optimizing Mounting Brackets (No. 2006-1-1480)*, SAE Technical Paper, <https://doi.org/10.4271/2006-01-1480>.
- Cho, S.S., Chang, H. and Lee, K.W. (2007) ‘Procedure for computer-aided preload selection of engine connecting-rod bolts’, *International Journal of Automotive Technology*, Vol. 8, No. 3, pp.319–325.
- European Committee for Standardization (2013) *Hot-Rolled Flat Products Made of High Yield Strength Steels for Cold Forming, Part 2: Technical Delivery Conditions for Thermomechanically Rolled Steels*, EN 10149-2. European Committee for Standardization, Brussels.
- Ghorpade, U.S., Chavan, D.S., Patil, V. and Gaikwad, M. (2012) ‘Finite element analysis and natural frequency optimization of engine bracket’, *International Journal of Mechanical and Industrial Engineering (IJMIE)*, Vol. 3, No. 2, pp.2231–6477.
- Gülbudak, K. and Yayla, P. (2009) ‘Development of a cornering bench fatigue test for the validation of a lightweight commercial vehicle front hub’, *Journal of Failure Analysis and Prevention*, Vol. 11, No. 5, pp.514–521, <https://doi.org/10.1007/s11668-011-9461-0>
- INTES GmbH (2012) *PERMAS Version 14 User's Reference Manual*. INTES Publications No. 450, Stuttgart, Germany.
- Kojima, Y. (2000) ‘Mechanical CAE in automotive design’, *R & D Review of Toyota CRDL*, Vol. 35, No. 4, p.1.
- Lonny, L., Thompson, L. and Chinnakonda, M. (2007) ‘Exact solution of time history response for dynamic systems with arbitrary viscous damping using complex modal analysis’, *ASME International Mechanical Engineering Congress and Exposition*, 11–15 November, Seattle, Washington, USA.
- Luizelli, M.C., Raz, D. and Sa’ar, Y. (2018) ‘Optimizing NFV chain deployment through minimizing the cost of virtual switching’, *IEEE INFOCOM 2018-IEEE Conference on Computer Communications*, pp.2150–2158, <https://doi.org/10.1109/INFOCOM.2018.8486315>
- Naghate, S. and Patil, S. (2012) ‘Modal analysis of engine mounting bracket using FEA’, *International Journal of Engineering Research and Applications (IJERA)*, Vol. 4, No. 2, pp.1973–1979.
- Paskalov, A. and Reese, S. (2003) ‘Deterministic and probabilistic floor response spectra’, *Soil Dynamics and Earthquake Engineering*, Vol. 23, No. 7, pp.605–618, [https://doi.org/10.1016/S0267-7261\(03\)00064-2](https://doi.org/10.1016/S0267-7261(03)00064-2)
- Polat, I. (2019) *Validation Studies on Dynamic Analysis Methodology of Polyethylene Fuel Tank Based on Test Results*, Istanbul Technical University, Graduate School of Science Engineering and Technology, Master’s Thesis.
- Raffaldini, C. (2012) *Structural Optimization in the Automotive Industry*, Master Thesis, University of Parma.
- Walunje, P. and Kurkute, V.K. (2013) ‘Optimization of engine mounting bracket using FEA’, *PARIPEX-International Journal of Research*, Vol. 2, No. 12, pp.1973–1979.
- Yang, R.J. (1991) ‘Shape sensitivity analysis and optimization using NASTRAN’, *Journal of Structural Mechanics*, Vol. 19, No. 3, pp.281–300, <https://doi.org/10.1080/08905459108905145>
- Yay, K. and Ereke, M. (2003) ‘A new approach for using road data in accelerated vehicle life tests’, *Itüdergisi/d Mühendislik*, Vol. 2, No. 5, pp.61–73.
- Zienkiewicz, O.C., Taylor, R.L. and Zhu, J.Z. (2013) *The Finite Element Method: Its Basis and Fundamentals*, Butterworth-Heinemann.

Websites

Entwicklung und Erprobung, Available from Internet: https://www.mercedes-benz-trucks.com/de_DE/models/new-actros/reliability.html (Accessed 26 February, 2021).

Long Distance Actros Chassis, Available from Internet https://www.mercedes-benz-trucks.com/en_ID/models/long-distance-actros/economics-and-technics/chassis.htm (Accessed 26 February, 2021).